PERGAMON

International Journal of Solids and Structures 36 (1999) 1845–1864

INTERNATIONAL JOURNAL OF SOLIDS and STRUCTURES

Global and local approaches to fracture normal to interfaces

A. S. Kim, J. Besson*, A. Pineau

Centre des Matériaux, Ecole des Mines de Paris, CNRS URA 866, BP 87 Evry, Cedex 91003, France

Received 8 September 1997; in revised form 2 February 1998

Abstract

The problem of a crack perpendicularly approaching a bimaterial interface is examined using both global and local approaches to fracture. The global approach is based on the *J*-integral with a second parameter, *Q*, which scales the stress triaxiality ahead of the crack. The local approach is based on either brittle fracture (Beremin model) or ductile fracture (Rice and Tracey model). In the first case, the Weibull stress over the plastic zone is calculated. In the second case, the void growth rate is calculated at the tip of the crack over a representative volume (generally associated with a characteristic length of the material). After a brief summary of each approach, the results for a crack near an elastically homogeneous, plastically mismatched interface are presented. The behaviour of the bimaterial is expressed in relation to the behavior of the homogeneous material. It is shown that there is an effect on the crack behavior which depends on the direction of crack propagation, i.e. from the harder material to the softer material or vice versa. This effect is examined as a function of change in yield strength ratio and hardening exponent, *n*. For the case of brittle fracture, the effect of changing the Weibull modulus, *m*, is also examined. The models based on the local approach show that both stress- and strain-controlled fracture mechanisms must be accounted for. This implies the necessity of using the two parameters *J* and *Q* in the global approach. This is due to the fact that the stress–strain fields ahead of the crack tip are affected by the nature of the second material.

1. Introduction

Numerous applications in which the fracture behaviour at interfaces must be considered can be found in the domains of the coating industry, composites, and the welding industries. Increasing interest in the application of functionally graded materials also requires a basic understanding of the effect of material property combinations on resistance to fracture.

Two common approaches to fracture in homogeneous materials are the global approach and the local approach. The global approach examines the change in the crack driving force in terms of the *J*-integral (Rice, 1968), which may be related to the energy release rate. More recently, the

* Corresponding author. Fax: 00 33 1 60 76 31 50; e-mail: besson@mat.ensmp.fr

0020–7683/99/$ - see front matter
PII: S0020–7683(98)00062–6

effect of the Q-factor (O'Dowd and Shih, 1991, 1992), which accounts for scaling the stress triaxiality depending on the crack tip constraint, has been emphasized. The second approach, referred to as the local approach, has been developed in particular by Beremin (1981, 1983) and considers the local near-tip stress and deformation contributions to the brittle and ductile failure processes. Both of these approaches have been applied to various fracture conditions in homogeneous materials and comparisons of the two approaches have been carried out by Pineau (1992) and Pineau and Joly (1991).

These two approaches may also be applied to the case of fracture in bimaterial systems. In bimaterial fracture, problem definition involves some basic features, namely the type of bimaterial system examined (elastic–elastic or elastic–plastic) and the orientation of the crack with respect to the interface (parallel or perpendicular). Once these conditions have been defined, the changes in crack driving force as a function of material properties and crack orientation may be examined using either the global or local approach.

The case of bimaterial fracture in elastic–elastic bimaterial systems has been studied by numerous groups for the crack both parallel and perpendicular to the interface. For the crack parallel to the interface of an elastic–elastic bimaterial, analytical results were first presented in Williams (1959) and England (1965). For the crack parallel to the interface of an elastic–plastic bimaterial numerical studies were reported by Woeltjen et al. (1993) and Ganti and Parks (1997). Experimental results using the local approach were presented by Ohata et al. (1996).

Fracture perpendicular to the interface has been studied by Zak and Williams (1963) for elastic–elastic bimaterials, and Romeo and Ballarini (1994, 1995) for elastic–plastic bimaterials. To the authors' knowledge, the case of a crack perpendicular to the interface has not yet been examined using the local approach.

The aim of the present work is to first re-examine the interfacial fracture problem for the crack perpendicular to the interface, using the two-parameter global approach to account for changes in crack tip triaxiality. Then, the same problem using the brittle and ductile failure models of the local approach is examined. The consequences of the bimaterial interface on fracture in terms of both the global and local approaches are presented and discussed. In particular, the bimaterial cases studied in this work may be applied, for example, to the case of welded austenitic and ferritic steels or heat-affected zones, which have similar elastic material properties but different plastic properties.

2. Problem formulation and finite element calculations

A schematic of the problem geometry and conventions is shown in Fig. 2. The crack is perpendicularly approaching the interface from material 1 towards material 2. The two materials have the same elastic moduli ($E_1 = E_2$), Poisson's ratio ($\nu_1 = \nu_2$), and hardening exponent but different yield strengths. The material law used to describe the behaviour is the power-law relation shown in eqn (1):

$$\varepsilon = \frac{\sigma_{Yi}}{E}\left(\frac{\sigma}{\sigma_{Yi}}\right)^{n_i} \tag{1}$$

where i refers to material 1 or 2. The yield strength ratio between the two materials is given by κ:

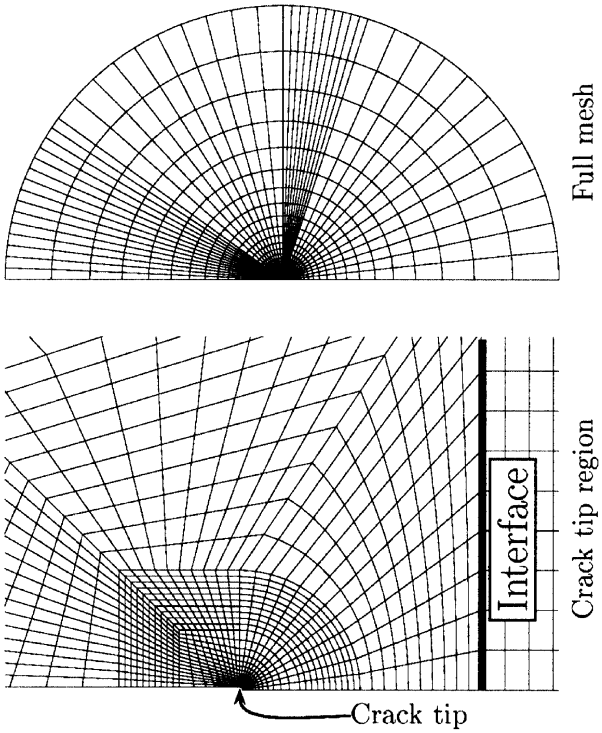

Fig. 1. Finite element full-scale mesh and crack-tip region.

$$\kappa = \frac{\sigma_{Y1}}{\sigma_{Y2}} \tag{2}$$

Five yield strength ratios are considered for three different hardening exponents. For material 1, $\sigma_{Y1}/E = 0.0015$ and $v_1 = 0.3$. The yield strength of material 1 remains fixed while the yield strength of material 2 varies to give a ratio $\sigma_{Y1}/\sigma_{Y2} = \frac{1}{2}, \frac{2}{3}, \frac{1}{1}, \frac{3}{2}$ or $\frac{2}{1}$. For a given bimaterial, the hardening exponent is the same for both materials and is taken to be $n = 2$, 10 or 100.

The crack is loaded by imposing a displacement along the edge of the mesh (Fig. 1) which is calculated from the elastic stress intensity factor (K-field) (see Fig. 2). Since the elastic moduli of the materials are the same, a change in the yield strength of the materials does not affect the loading required on the far-field boundaries as long as the conditions of small-scaled yielding are fulfilled. Thus, the material response at the tip of the crack can be compared for different yield strength combinations subjected to the same far-field loading conditions.

Under small-scale yielding conditions, the J-integral can be related to the elastic K field by the following relation:

$$J = \frac{K^2}{E}(1-v^2) \text{ plane strain}; \quad J = \frac{K^2}{E} \text{ plane stress} \tag{3}$$

The characteristic length scale used in this problem is $r_c = J/\sigma_{Y1}$. A finite deformation zone exists

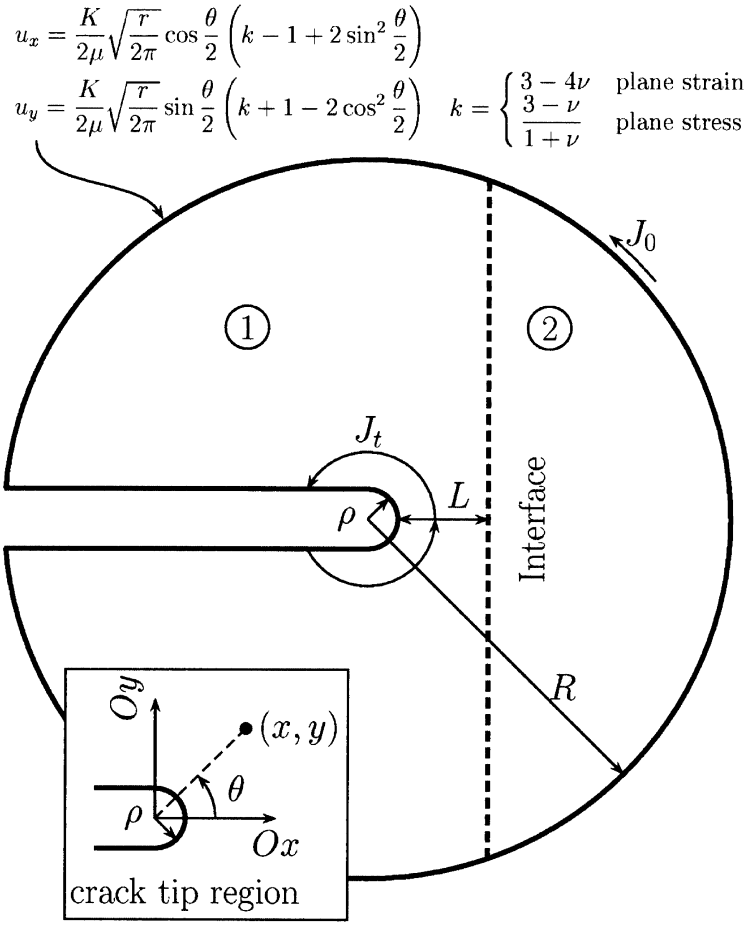

Fig. 2. Schematic showing problem geometry and conventions.

ahead of the crack tip within approximately $2r_c$ (O'Dowd and Shih, 1991, 1992). Outside of this zone, the HRR (Hutchinson–Rice–Rosengren) fields (Hutchinson, 1968; Rice and Rosengren, 1968) characterize the near-tip stress and deformation fields ahead of the crack. The r_c at the maximum load, $r_c^{\max} = J^{\max}/\sigma_{Y1}$, is used to define the second length scale, $L \simeq 4r_c^{\max}$, which is the length from the crack tip to the interface. This value is used to normalize the load parameter giving $J_0/\sigma_{Y1}L$. Note that if L is too large, there is no interaction between the plastic zone and the interface. Thus, the crack is essentially still in a homogeneous material. Conversely, if L is too small the crack is essentially on the interface and the effect of the interface ahead of the crack is limited. Here, L is chosen to be smaller than the plastic zone size at the maximum load. Typical values used for steels are: $\sigma_Y = 300$ MPa, $n = 10$, $L = 1$–5 mm, and $J_{\mathrm{Ic}} = 200$ kJ/m^2. In the present study, the following combinations were used in order to represent a wide range of material properties: $\kappa = \frac{1}{2}, \frac{2}{3}, \frac{1}{1}, \frac{3}{2}, \frac{2}{1}$, $n_1 = n_2 = n = 2, 10, 100$.

Finite element calculations were carried out using the finite element code Zébulon (Foerch et

al., 1997; Besson and Foerch, 1997). The mesh consists of approximately 2600 eight-noded elements using reduced integration. The notch root radius at the tip of the crack is $\rho \simeq \frac{1}{20} r_c^{\max}$. The calculations were carried out in small-deformation using a Newton–Raphson integration scheme. The J-integral was computed using the DeLorenzi volume integral (DeLorenzi, 1985).

3. Global approach

3.1. J-integral

In the global approach, the J-integral is used to evaluate the crack driving force at the tip of the crack as a function of the far-field loading, K. Under small-scale yielding in a homogeneous material, J can be determined from K by the relation given in eqn (3). In a homogeneous material, a contour near the crack-tip or on the far-field boundary will give the same value for J. For a bimaterial, however, although the far-field integral does not change, there is a change in the near-tip J (see Fig. 2), referred to as J_t, since the deformation and stress fields are affected due to the presence of the second material.

In order to evaluate the effect of the second material for a bimaterial subjected to a given K field, the J-integral taken at the tip of the crack in the bimaterial, J_t, is compared to the J-integral of the homogeneous material, J_t^h, which has been submitted to the same external loading conditions. If the ratio J_t/J_t^h is greater than one, this indicates an increase or 'amplification' in the crack-tip driving forces. If the ratio is less than one, this is referred to as a 'shielding' effect.

3.2. Modified HRR-field

The J-integral can be used to express the near-tip deformation and stress fields through the use of the HRR-fields (Hutchinson, 1968; Rice and Rosengren, 1968). Under certain conditions, such as a semi-infinite crack in an infinite (homogeneous) body, the stress and strain profiles given by the HRR-fields are close to the full-field solution. Under other conditions, however, a second term must be used to scale the crack tip stress fields. An example of such a situation can be found in the case of full-scale plastic yielding, as may occur in finite specimen geometries, or for cracks near interfaces.

A Q-term, introduced by O'Dowd and Shih (1991, 1992), is used as the scaling factor which scales the triaxial field ahead of the crack relative to a high or low triaxial reference field. Using the HRR field as the reference field in a homogeneous material with yield strength σ_Y, for example, Q is defined as:

$$Q = \frac{\sigma_{\theta\theta} - (\sigma_{\theta\theta})^{\mathrm{HRR}}}{\sigma_Y} \tag{4}$$

at $\theta = 0$, $r \simeq 2r_c$, where θ is the angle from the crack plane and r is the radial distance from the crack tip. The length $r \simeq 2r_c$ delimits the region outside of which this field may be evaluated. The stress triaxiality scaling factor near the crack tip for a given bimaterial under a given load is referred to as Q_t. Note that for the results presented in Sections 5.1.2 and 5.1.3, the value of Q_t is

taken at $r \simeq 2r_c \geqslant 3\rho$, thus insuring that we have a valid Q value which has been obtained outside of the finite deformation zone.

The Q term may be incorporated into the stress field expression by using a modified HRR field:

$$\frac{\sigma_{ij}}{\sigma_Y} = \left(\frac{JE}{\sigma_Y^2 I_n r}\right)^{1/(n+1)} \tilde{\sigma}_{ij}(\theta, n) + Q\delta_{ij} \tag{5}$$

Here, I_n is the integration constant, which was determined numerically and $\tilde{\sigma}_{ij}(\theta, n)$ is a dimensionless angular function, where δ_{ij} is the Kronecker delta. Both can be found in (Shih, 1983). Note that Q is assumed to be independent of r.

The strain is given by:

$$\frac{\varepsilon_{ij}}{\varepsilon_Y} = \left(\frac{JE}{\sigma_Y^2 I_n r}\right)^{n/(n+1)} \tilde{\varepsilon}_{ij}(\theta) \tag{6}$$

where $\tilde{\varepsilon}_{ij}(\theta)$ is also given in (Shih, 1983). It is important to note the role of J and Q in the stress expression given for σ_{ij}/σ_Y as well as the relative change in σ_{ij}/σ_Y and $\varepsilon_{ij}/\varepsilon_Y$ with increasing n. For large n and with increasing load, the first term of eqn (5) increases at a rate slower than that of the second term. At small n, however, the first term becomes more significant.

Upon considering the expression in eqn (6), we see that the $\varepsilon_{ij}/\varepsilon_Y$ term is to the power $n/(n+1)$. Since the term

$$\left.\frac{JE}{\sigma_Y^2 I_n r}\right|_{r=2r_c} = \frac{E}{2I_n\sigma_Y}$$

is greater than one, the contribution of deformation to a criterion which considers both stress and deformation will increase faster than the contribution of stress, which is only to the power $1/(n+1)$. These points will be important for the discussion of results in Section 5.1.3.

An increase or decrease in the triaxial stress results in a stronger or weaker driving force, respectively, for the crack. Since varying degrees of triaxiality can exist for the same degree of deformation at the crack tip, two different bimaterials with the same J_t value will not necessarily have the same Q_t. Note that for the results presented in Section 5.1.3, the Q_t values are calculated based on the near-tip stress fields calculated from J_t (not the remote boundary J).

One example of the effect of Q, examined by O'Dowd and Shih (1991, 1992), is in the presence of full-scale plastic yielding. In their work, they show that depending on specimen geometry, different levels of constraint are induced for the same far-field K.

4. Local approach

4.1. Beremin brittle fracture model

The brittle fracture model developed by Beremin (1983) may be used to determine the probability of fracture for a brittle material. The theory is based on a critical stress theory and also takes into account the contribution of the Weibull effect in which the probability of reaching the critical

stress is greater for a greater volume sample, thus incorporating the statistical aspects of brittle fracture.

The Weibull stress, σ_w, is obtained by integrating the maximum principal stress, σ_I, over a plastically deformed volume:

$$\sigma_w = \left(\frac{1}{V_0} \int_{V, p > p_c} \sigma_I^m \, \mathrm{d}V \right)^{1/m} \tag{7}$$

Here, V_0 is the elementary unit volume, V is the volume over which the plastic deformation, p, is greater than a critical plastic deformation, p_c, and m is the Weibull modulus.

The probability of fracture is then given by:

$$P_r = 1 - \exp\left[- \left(\frac{\sigma_w}{\sigma_u} \right)^m \right]. \tag{8}$$

Note that only two parameters are needed to describe the material: $\sigma_u^m V_0$, where σ_u is the critical stress required to fracture a volume, V_0, and m, the Weibull modulus. Note also that the choice of the volume V_0 is not significant since the results are always presented in terms of the ratio $\sigma_w/\sigma_w^{\mathrm{h}}$, where σ_w^{h} is the value of the Weibull stress computed for the homogeneous material.

4.2. Modified Rice and Tracey ductile fracture model

Void growth ahead of the crack tip is given by the Rice and Tracey (Rice and Tracey, 1969) ductile fracture model. The modified version used by Beremin (1981) incorporates strain hardening effects into this model. Void growth is determined by integrating a term incorporating the plastic deformation and stress triaxiality over a characteristic volume, once again related to a characteristic length of the material ahead of the crack. For this model, the characteristic distance is taken as $\lambda_c \simeq L/4 \simeq r_c^{\max}$ and is used to define the volume over which the integral shown in eqn (9) is evaluated. Using the material values and definition of r_c given in Section 2, $r_c = \mathrm{J}/\sigma_Y = \lambda_c \simeq 200$–500 microns which is on the order of the inclusion spacing in a typical material.

According to the model for ductile fracture, failure occurs when the void growth ratio reaches a critical value, $(R/R_0)_c$. The void growth is related to the stress triaxality ratio, σ_m/σ_{eq}, and plastic deformation by the equation:

$$\ln\left(\frac{R}{R_0} \right) = \int_{\varepsilon_d}^{\varepsilon_{eq}} 0.283 \exp\left[1.5 \left(\frac{\sigma_m}{\sigma_{eq}} \right) \right] \mathrm{d}\varepsilon_{eq} \tag{9}$$

where R and R_0 are the final and initial radius, respectively, of the void, ε_{eq} is the cumulative plastic strain, ε_d is the deformation necessary to nucleate cavities from inclusions, and σ_m and σ_{eq} are the mean stress and the equivalent stress (Von Mises stress), respectively. The integral is taken over a volume of dimensions $\lambda_c \times \lambda_c \times$ unit thickness. In the following, it is assumed that $\varepsilon_d = 0$ for the sake of simplicity.

4.3. Strain control fracture model

A third local criterion can be developed based on the cumulative plastic strain averaged over a given volume: $\varepsilon_{\mathrm{p}}^{\mathrm{cum}}$. Here, the volume over which $\varepsilon_{\mathrm{p}}^{\mathrm{cum}}$ is determined has the same dimensions as

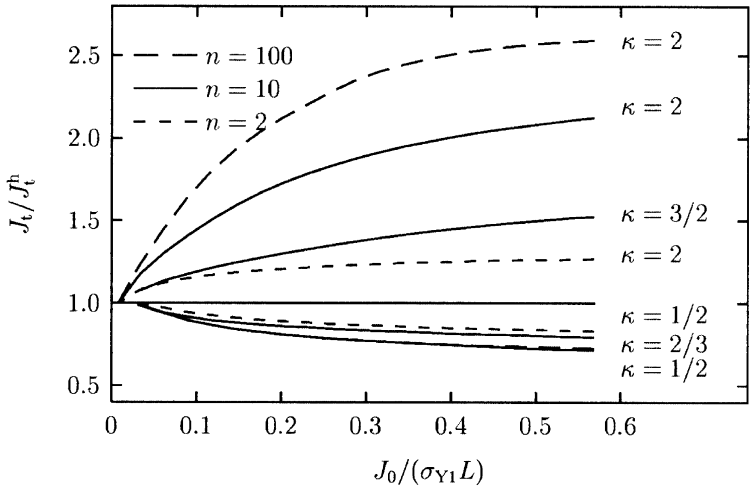

Fig. 3. Variation in normalized J_t as a function of normalized load for various κ and n (plane strain).

that used for the ductile failure model used in Section 4.2. Since this model is solely deformation based, it is used here for comparison to the results of the J-integral.

5. Results and discussion

We now consider the numerical results obtained using each of these approaches. We begin with the results in terms of the global approach, first with the J-integral alone, and then with Q. We then consider the local approach using first the brittle model and finally the ductile model.

5.1. Global approach

5.1.1. J-*integral*

As discussed in Section 3.1, the J-integral is used to evaluate the crack driving force at the tip of the crack. In particular, the ratio J_t/J_t^h is used to determine if there is an increase or decrease in the crack tip driving force due to the presence of the second material. We begin with the case of a bimaterial with varying κ and n, shown in Fig. 3. The stress rate is plane strain and the results are presented in terms of the normalized load parameter, $J_0/\sigma_{Y1}L$, vs the changes in crack-tip driving force, J_t/J_t^h.

For $\kappa > 1$, the crack approaches the interface from the harder material and the ratio J_t/J_t^h is greater than one, indicating an increase or 'amplification' in the crack driving force. Note again that this is the plane strain state. For a given κ, the amplification effect is stronger for larger n, and for a given n, increases with increasing κ. These effects can be understood in terms of a change in the degree of deformation at the crack tip. The softer the material on the other side of the interface, the lower the constraint and thus the greater the deformation at the crack tip compared to the homogeneous material. The reverse effects are true for $\kappa < 1$ (soft to hard) with stronger shielding effect for increasing n and for decreasing κ. These effects, however, are less pronounced than for

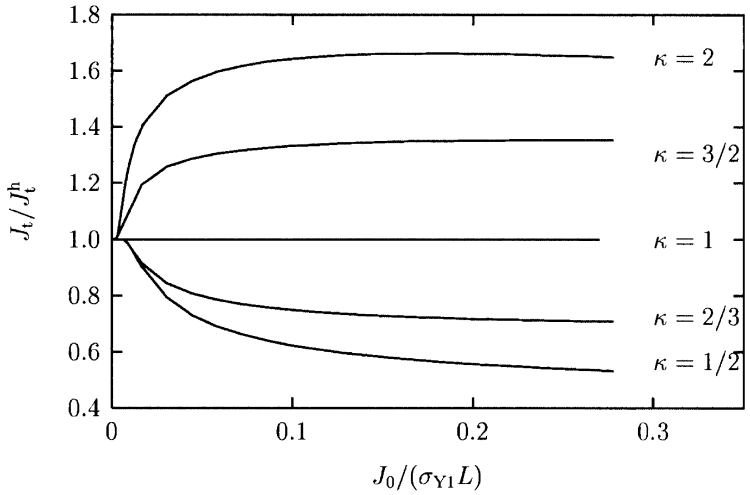

Fig. 4. Variation in normalized J_t as a function of a normalized load for various κ with $n = 10$ (plane stress).

$\kappa > 1$ since the addition of the harder material constrains the relative amount of deformation possible compared to the homogeneous material.

The results for the plane stress case for $\kappa = 2$, 1.5, 0.66 and 0.5 and $n = 10$ are shown in Fig. 4. The general behaviour is similar to those found for the plane strain case, with amplification when the crack approaches the interface from the harder material and shielding when approaching from the softer material.

The results shown in Figs 3 and 4 indicate that, in general, there is an 'amplification' effect of the driving forces when the crack propagates from hard to soft and a 'shielding' effect when the crack propagates from soft to hard. These results are consistent with those reported in Sugimura et al. (1995) and Kim et al. (1997).

The use of J_t as the sole crack driving force criterion is sufficient when the conditions of J-dominance are fulfilled. In the case of a bimaterial however, additional constraints due to the presence of the second material may result in a deterioration of the J-dominant state. It is thus prudent to compare the stress profile ahead of the crack to the HRR field to determine whether or not the constraint due to the second material is significant.

5.1.2. Q-*factor*

Figure 5 shows the stress triaxiality contours ahead of the crack tip and their corresponding plastic deformation zones according to calculations for the homogeneous material ($\kappa = 1$) and the bimaterials $\kappa = 2$ and 0.5. The hardening exponent for all three cases is $n = 10$. These plots are for the same J_t at the crack tip (thus not necessarily the same far field load). It can be clearly seen that the triaxiality at a given J_t is not the same for the three cases.

Figure 6 shows a plot of the opening stress profile ahead of the crack for the same material systems shown in the previous figure. The HRR field for a homogeneous material is indicated by the dashed line. The stress profiles are again given for the same J_t value. It can be seen that, depending on the crack propagation direction, from hard to soft or soft to hard, there is a decrease

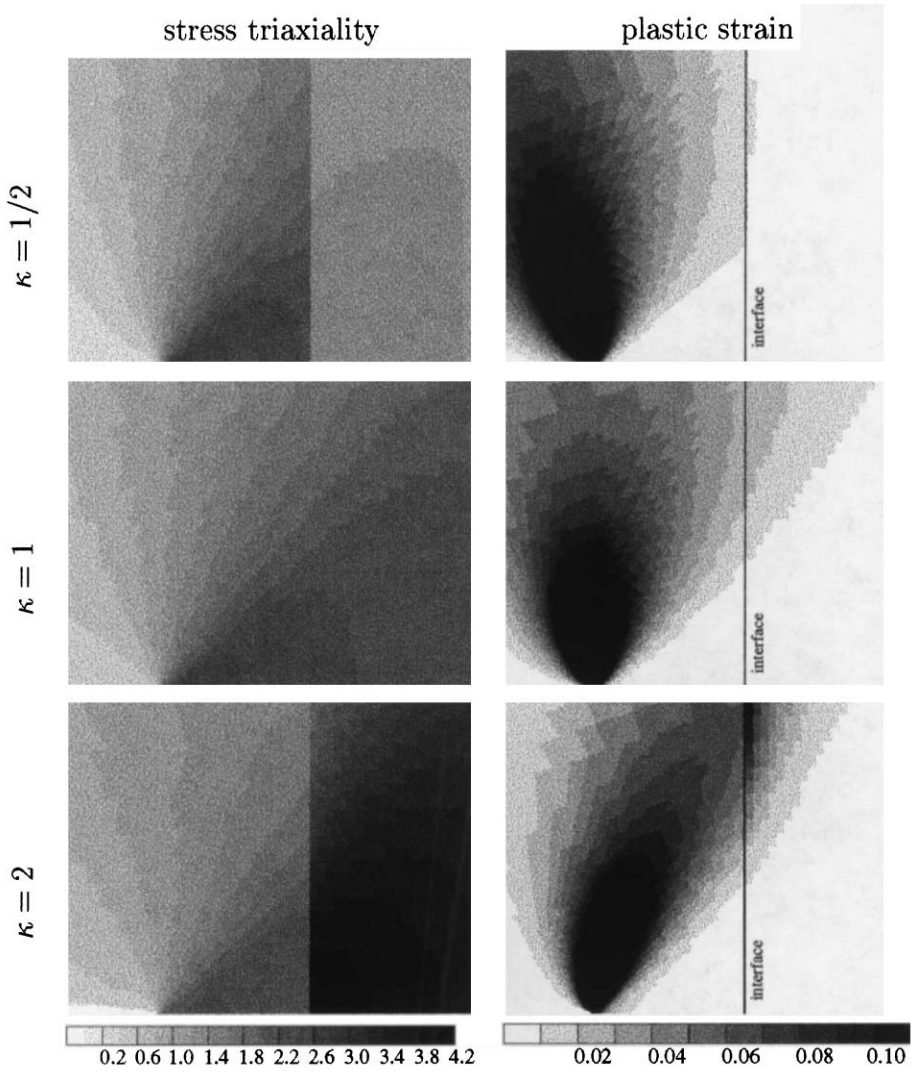

Fig. 5. Values of stress triaxiality at Gauss points and their corresponding plastic deformation zones for different values of κ with $n = 10$ for $J_t/\sigma_Y L = 0.3$.

or increase, respectively, in the opening stress field ahead of the crack compared to the homogeneous material. These trends, in terms of increasing the probability for fracture, are the reverse of those observed for the deformation based J-integral (Fig. 3).

In the same manner that the constraint due to the second material has an effect on the degree of deformation, as expressed by J_t, the difference in stress profiles is also a result of the constraint due to the second material. The constraint effect on the stress state is expressed by Q, defined in eqn (4). Recall that a positive Q indicates an increase in the stress triaxiality, thus increasing the failure probability, and a negative Q indicates a decrease in the stress triaxiality, decreasing the

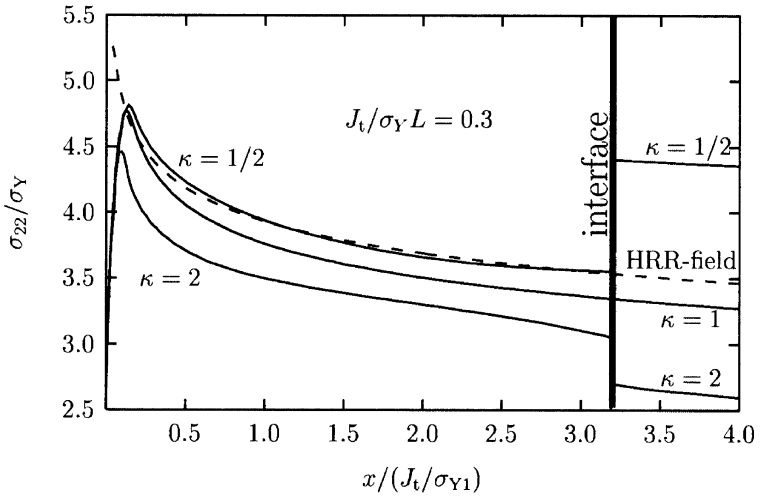

Fig. 6. Normalized opening stress profile for homogeneous and bimaterials for $\kappa = 2$, 0.5 ($n = 10$). The dashed lines indicate the HRR-field.

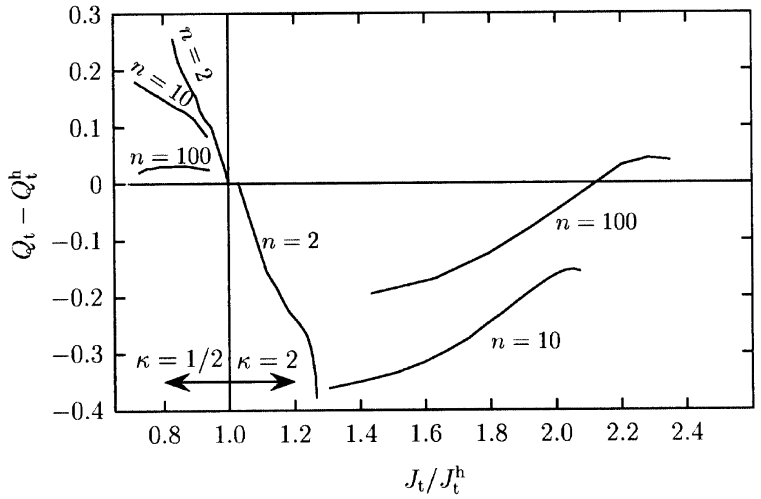

Fig. 7. Change in J and Q (both expressed in relation to homogeneous material) for various n ($\kappa = 2$, 0.5).

failure probability. Note that this difference can be significant if the value of Q_t^h is on the order of ± 0.5.

5.1.3. *Combined effects of* J *and* Q

Now, having presented the principles of the interface effect on crack driving force in terms of J and Q, it is interesting to consider the two effects simultaneously for several bimaterial combinations. Such a plot is shown in Fig. 7. Here, we see the change in J_t/J_t^h and $Q_t - Q_t^h$ for fixed κ

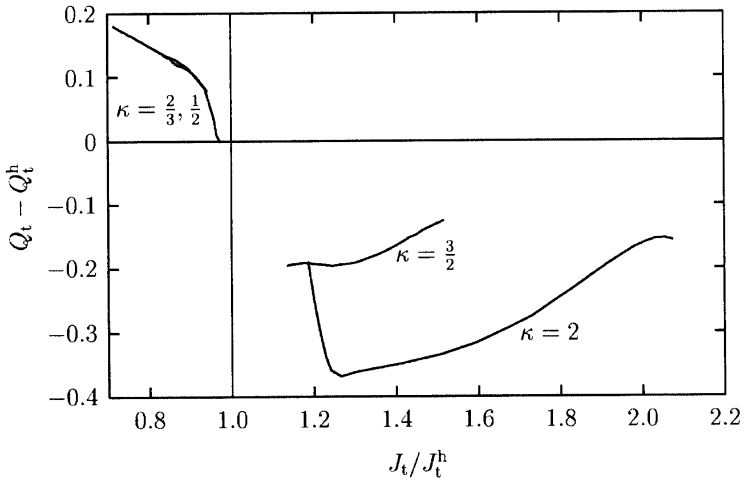

Fig. 8. Change in J and Q (both expressed in relation to homogeneous material) for various κ ($n = 10$).

and varying hardening exponent. The stress state is plane strain. Note that the x-axis in this figure is given in terms of the actual crack tip state, J_t/J_t^h, instead of the far-field load, $J_0/\sigma_{Y1}L$, in order to compare Q_t for the crack subjected to the same J in the two materials.

It is useful to divide this $(J_t/J_t^h)-(Q_t-Q_t^h)$ space into four quadrants, each of which corresponds to a particular crack-tip state. In the upper-right quadrant, $J_t/J_t^h > 1$ and $Q_t-Q_t^h > 0$. Since both conditions individually lead to increased chances for failure, it is reasonable to assume that an increase in both will also facilitate fracture. This is obviously an undesirable region of the $(J_t/J_t^h)-(Q_t-Q_t^h)$ space. The lower-left quadrant in which $J_t/J_t^h < 1$ and $Q_t-Q_t^h < 0$ indicates the reverse tendencies, reducing the crack-driving force and the initial stress state. Thus, in terms of materials design it would be advantageous to have bimaterials whose properties fall into this quadrant of the plot.

Conclusions pertaining to fracture states which fall into the remaining two quadrants are less obvious. The results presented for the bimaterials considered in the present work fall into these quadrants and thus the relative importance of the J and Q criteria must be evaluated in order to define regions delimiting the chances for failure.

Returning to the numerical results presented in Fig. 7, we see that for $\kappa < 1$, there is a continuous increase in $Q_t-Q_t^h$ for a given κ and for decreasing n. For $\kappa > 1$ there is an increase or decrease in $Q_t-Q_t^h$ depending on the hardening exponent. Note that for the values at low loads (J_t/J_t^h close to one), Q cannot be evaluated since the distance at which Q is evaluated is of the same order of magnitude as the crack radius, ρ.

The same plot for varying κ and $n = 10$, which is a value relevant to common materials, is shown in Fig. 8 again for the plane strain case. It can be seen that for $\kappa > 1$, there is an increase in J_t/J_t^h and a decrease in $Q_t-Q_t^h$ for increasing κ. Practically no difference is observed for the two cases where $\kappa < 1$.

Similar plots for the plane stress case are shown in Fig. 9. These trends are consistent with those found in the plane strain case, though the $Q_t-Q_t^h$ effect is significantly weaker. In fact, they are

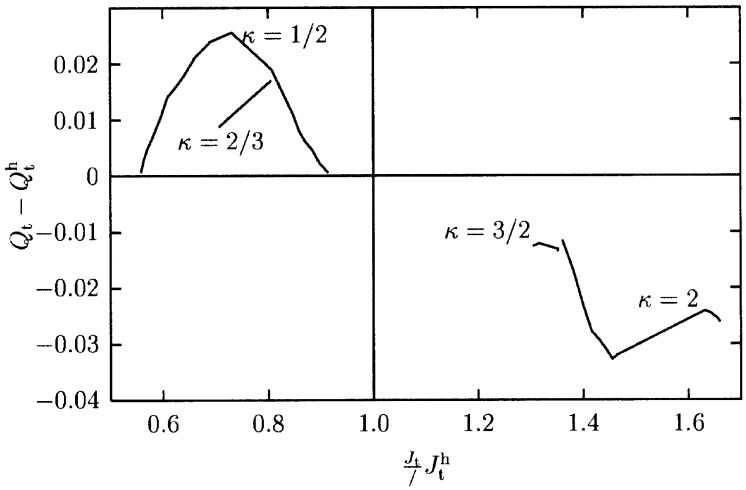

Fig. 9. Change in J and Q (both expressed in relation to homogeneous material) for various n ($\kappa = 2$, 0.5 plane stress).

almost non-existent since the constraint effect in the out-of-plane direction no longer exists. The ability of the material at the interface to relax despite an increase in load reduces the change in stress triaxiality.

It is clear that, especially in the case of plane strain, both the J and Q conditions must be considered to fully capture the effect of the second material on the crack driving force. It appears that the Q criterion is less important in the plane stress case due to the relaxation of stresses at the material interface.

5.2. Local approach

The local approach provides another method by which the difference according to a stress-based or stain-based model may be clearly illustrated. We first examine the results obtained using the deformation-based cumulative plastic strain to measure the change at the crack tip, then using the brittle model (stress-controlled) and finally, the ductile model (deformation/stress triaxiality controlled).

5.2.1. Strain-controlled model

Figure 10 shows the $J_0/\sigma_{Y1}L$ vs $\varepsilon_p^{cum}/\varepsilon_p^{h,cum}$ for various κ and n. The criterion, ε_p^{cum} is based on the average plastic deformation over the characteristic volume discussed in Section 4.2. Since it is based solely on the deformation at the tip of the crack, this criterion gives the same trends as those given by the J_t/J_t^h criterion (Fig. 3). Namely, an increased chance for failure compared to the homogeneous ($\kappa = 1$) material if the crack propagates from hard to soft and a decreased chance if the crack propagates from soft to hard. The ratio, $\varepsilon_p^{cum}/\varepsilon_p^{h,cum}$ is related to J_t by:

$$\frac{\varepsilon_p^{cum}}{\varepsilon_p^{h,cum}} \simeq \left(\frac{J_t}{J_t^h}\right)^{n/(n+1)}$$

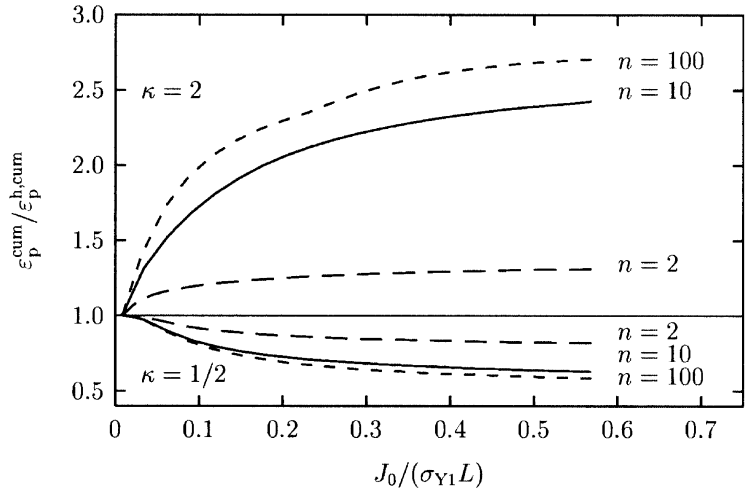

Fig. 10. Normalized cumulative plastic deformation (ε_p^{cum}) as function of normalized load for various n (plane strain).

for high J_t, i.e. when the zone defined by the characteristic length λ_c is fully yielded which agrees with eqn (6).

5.2.2. Model for brittle failure

Recall from Section 4.1 that the local approach brittle fracture model is based on a Weibull stress criterion integrated over a plastically deformed volume of material ahead of the crack tip. In the results presented here, σ_w for the material in which the crack resides was measured and compared to σ_w^h of the corresponding section in the homogeneous material in order to evaluate the effect of the interface on fracture properties. It is pointed out here that since σ_w of the second material was not considered, the possibility of failure occurring in the second material before the crack interacts with the interface was not considered.

The brittle model applied to the bimaterial case where $n = 10$ and the yield strength ratio varies as 0.5, 0.66, 1.5 and 2 is shown in Fig. 11. For $\kappa = 2$ at low loads, we see that the presence of the second material initially induces a shielding effect compared to the homogeneous material. As the far-field load increases, the ratio σ_w/σ_w^h increases and eventually becomes greater than one, indicating an amplification effect due to the presence of the second material. Note that even small values of σ_w/σ_w^h, when considered in terms of failure probability, can be significant since they are taken to the power of the Weibull modulus, m.

The behaviour of this curve can be explained by recalling that the model for brittle fracture is based on an integral over a volume for which $p > p_c$. In these calculations, p_c was taken to be 0.001. There are two factors which contribute to the evolution of the σ_w/σ_w^h curve. At low loads, the stress dominating criterion, related to the maximum principal stress, governs the behaviour. With increasing loads, as the yielded zone grows, the deformation part of the failure process, associated with the plastic zone size, begins to dominate.

The tendencies corroborate the results observed in Section 5.1, where the two terms J_t/J_t^h and $Q_t - Q_t^h$ give opposite results for the same bimaterial case. Note that the evolution of both of these

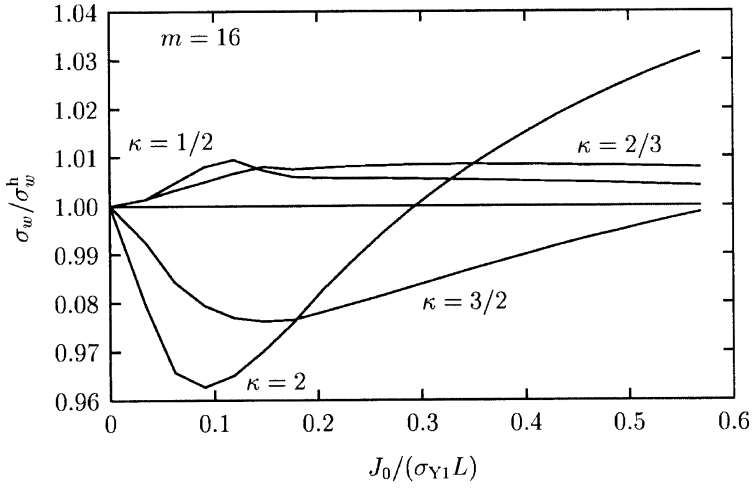

Fig. 11. Variation in normalized Weibull stress as a function of normalized load for $n = 10$, $m = 16$.

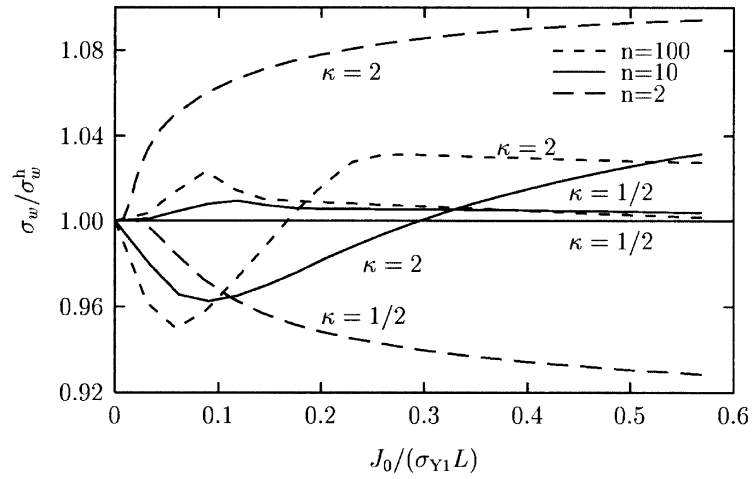

Fig. 12. Variation in normalized Weibull stress for various n ($\kappa = 2, 0.5$).

criteria as a function of increasing load is the same (both increasing). Similar results are obtained for $\kappa = 3/2$.

Consider now the case of $\kappa = 2$, $n = 2$, shown in Fig. 12. Based on the results for $n = 10$, we would expect a similar evolution of the σ_w/σ_w^h curve, with Q dominating at lower loads and J becoming more significant at higher loads. Here, however, we see that the evolution of results resembles those obtained for the J_t/J_t^h criterion : a continuously increasing chance for failure when the crack approaches the interface from hard to soft and a decreasing chance for failure when the crack propagates from soft to hard. There is no longer the variation from shielding to amplification

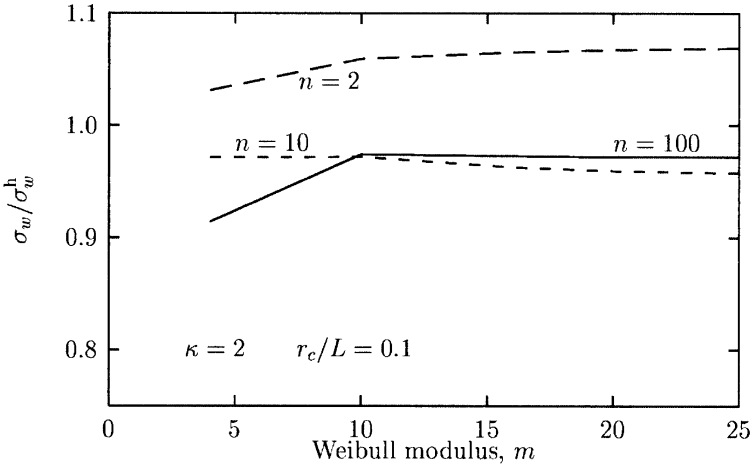

Fig. 13. Change in σ_w/σ_w^h for various m at low J_t.

observed for $\kappa = 2$ and $n = 10$. This can be understood by again considering the modified HRR field.

We see in eqn (5) that two terms contribute to the stress field profile. As a result of the constraint imposed by the second material, these two terms result in competing effects for a given bimaterial and loading system. The opposing effects arise from the fact that the J term is a deformation related criterion while the Q term is solely a stress-based criterion, each of which reacts differently under imposed constraint conditions. The dependence of the ratio σ_w/σ_w^h on these two effects can be seen by considering the role of the hardening exponent, n.

The relative importance of the first term of the modified HRR field is clearly dependent on the value of the hardening exponent, n. Depending on if n is large or small, the J term is more or less significant compared to the Q term. This explains the varying response of the σ_w/σ_w^h criterion despite a monotonically increasing external load. For high n ($n = 10$, 100) the Q-based part of the stress field becomes more important. The behaviour therefore generally follows that of the Q criterion discussed in Section 5.1.2, until, at higher loads, the effect of the large yielded volume emerges and increases σ_w/σ_w^h.

Similar plots for σ_w/σ_w^h as a function of m are shown in Figs 13 and 14,, for low ($r_c/L = 0.1$) and high ($r_c/L = 0.57$) loads, respectively. In both cases, the ratio σ_w/σ_w^h is relatively constant for $m \geqslant 10$. For $4 \leqslant m \leqslant 10$, there is a dramatic change for the hardening exponent $n = 100$ at both low and high loads and for $n = 10$ at high loads. There is relatively little change for $n = 2$ at low and high loads and for $n = 10$ at low loads. Typical values of m for average steels fall between $15 \leqslant m \leqslant 25$. For brittle materials, m values can be much lower but the hardening behaviour is strong so the effect of m is expected to be low.

The same bimaterials examined under plane-stress conditions show results similar to those found with the J-integral criterion alone (Figs 3 and 4). That is, an increase in the Weibull stress for the crack propagating from hard to soft and a decrease for the crack propagating soft to hard. This corresponds well with the results found for $J_0/\sigma_{Y1}L$ vs $Q_t - Q_t^h$ in the global approach, where the $Q_t - Q_t^h$ value was almost zero.

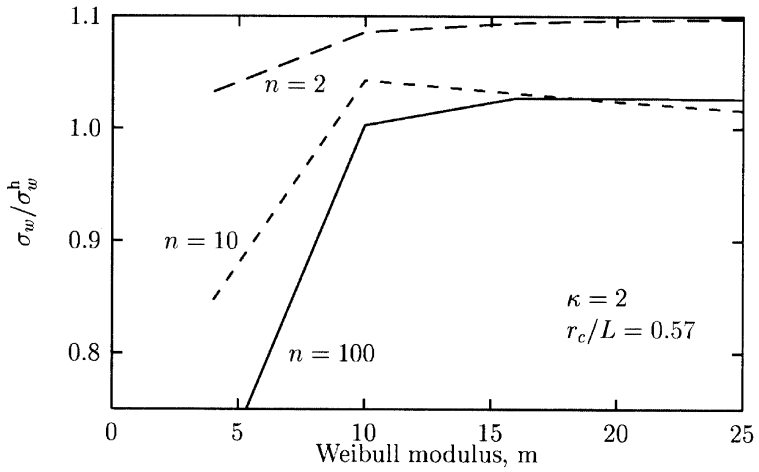

Fig. 14. Change in σ_w/σ_w^h for various m at high J_t.

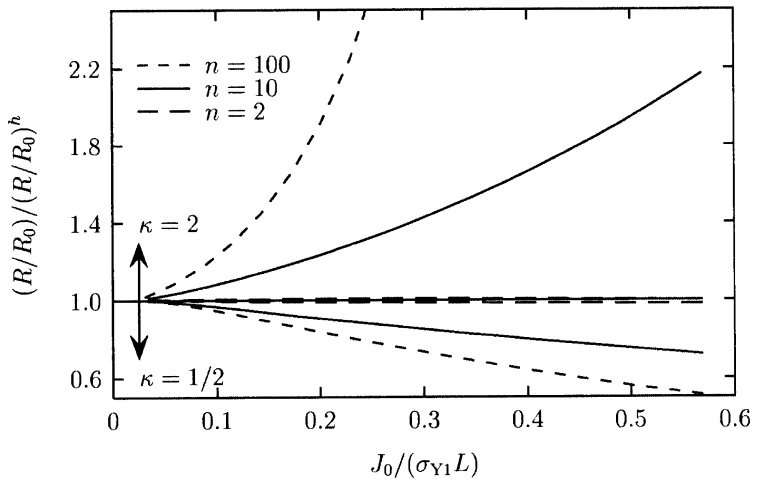

Fig. 15. Variation in normalized ductile rupture parameter $(R/R_0)/(R/R_0)^h$ as a function of normalized load for various n ($\kappa = 2, 0.5$).

5.2.3. Model for ductile fracture

The change in fracture behaviour according to the ductile failure model is examined in this section. Recall from Section 4.2 that the ductile failure model is based on the attainment of a critical void growth ratio in a characteristic volume ahead of the crack tip. In order to study the influence of the interface on the void growth ratio, we consider the ratio of (R/R_0) measured for the bimaterial compared to that of the homogeneous material, $(R/R_0)^h$, for the same far-field loading conditions. Recall from Section 4.2 that $\lambda = L/4$.

In Fig. 15 we see $(R/R_0)/(R/R_0)^h$ vs $J_0/\sigma_{Y1}L$ for the bimaterial case with $\kappa = 0.5$, 2 and $n = 2$, 10, 100. Note that R_0 in (R/R_0) and $(R/R_0)^h$ is the same since it refers to the initial cavity size in

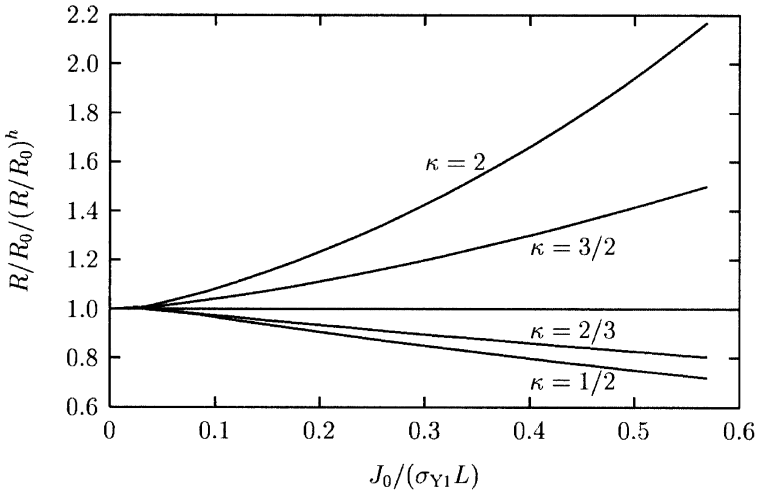

Fig. 16. Variation in ductile rupture parameter as a function of normalized load for various κ ($n = 10$).

the undeformed material. When the crack propagates from hard to soft, there is an increase in the void growth compared to the homogeneous material, indicating that fracture occurs earlier than in the homogeneous material. A decrease in this ratio is observed when the crack approaches the interface from the softer material towards the harder material. The change in the latter case is less pronounced than that of the former. This is reasonable since the degree of deformation constraint imposed by the harder material on the softer material is less than in the reverse case (see Fig. 10). Larger variations in the $(R/R_0)/(R/R_0)^h$ ratio are observed for material with low hardening for both shielding and amplification conditions.

$(R/R_0)/(R/R_0)^h$ for $n = 10$ and varying κ is shown in Fig. 16. The results correspond well with those expected based on a deformation-based criterion, with stronger amplification as the κ ratio increases above one or stronger shielding as κ decreases below one.

The results found for the ductile model correspond well with those found in the global approach using J alone, except for the case of $n = 2$, where practically no change in $(R/R_0)/(R/R_0)^h$ is observed. The difference between the two models can be explained by the consideration of the triaxial stress effect in the local approach for ductile fracture. Note that in all cases considered here, the decrease of stress triaxility is not high enough to overcome the increase in plastic deformation.

6. Summary and conclusions

The problem of a crack perpendicularly approaching a bimaterial with different yield strengths ($\sigma_{Y1} \neq \sigma_{Y2}$) and the same hardening exponent ($n_1 = n_2$) has been examined in the context of both global and local approaches to fracture. It is shown that the beneficial or detrimental effect due to the presence of the second material may be evaluated according to either a stress- or strain-based criterion.

In the global approach, it has been shown that if a stress based criterion describes the failure

mode, the single parameter J is not sufficient, and the two-parameter (J–Q) approach must be used in order to fully describe the effect of the bimaterial interface on crack propagation. This is due to the role of the triaxial stress in influencing the maximum stress over a characteristic distance. The exception to this approach is in the case of a bimaterial under plane stress conditions where the change in triaxiality with increasing load is close to zero.

In the global approach, if deformation alone describes the failure process, (such as in the case of plane stress) the J-integral alone provides results similar to those based on the ductile model of the local approach.

A careful analysis of the relative importance of the J and Q parameters must be carried out to understand the implications of an interface with respect to fracture resistance. Namely, a criterion which delimits the boundary within J–Q space outside of which fracture occurs would be useful for materials design. Such an approach for homogeneous materials has already been examined by Dodds et al. (1993).

The local approach provides one means of separating the deformation vs stress-based fracture criteria for specific cases. Depending on if the material fails by a brittle or ductile fracture mechanism, changes in the propensity to fracture can be evaluated as a function of bimaterial mismatch properties. The brittle fracture model, based on the Weibull approach, provides results similar to the J-integral criterion for materials with high hardening ($n = 2$–4). That is, an amplification effect as the crack approaches the interface from the harder material. For materials with lower hardening, however, there is an evolution of the σ_w/σ_w^h value depending on the degree of loading. For materials with a hardening exponent $n = 10$, for example, the model seems to indicate a small shielding effect at low loads for the crack approaching the interface from the harder material and then less shielding as the load increases. The ductile fracture model, which is based on cavity growth, exhibits trends similar to the J-integral for all κ and n considered in this study.

Acknowledgement

The authors are grateful to the Ministére des Affaires Etrangéres (France) for financial support for A.S.K.

References

Beremin, F., 1981. Cavity formation from inclusions in ductile fracture. Met. Trans. 12A, 723–731.

Beremin, F., 1983. A local criterion for cleavage fracture of a nuclear pressure vessel steel. Met. Trans. 14A, 2277–2287.

Besson, J., Foerch, R., 1997. Large scale object oriented finite element code design. Computer Methods in Applied Mechanics and Engineering 142, 165–187.

DeLorenzi, H.G., 1985. Energy release rate calculations by the finite element method. Eng. Fract. Mech. 21 (1), 129–143.

Dodds, R., Shih, C., Anderson, T., 1993. Continuum and micromechanics treatment of constraint in fracture. Int. J. Fract. 64, 101–133.

England, A., 1965. A crack between dissimilar media. J. Appl. Mech. 32, 400–402.

Foerch, R., Besson, J., Cailletaud, G., Pilvin, P., 1997. Polymorphic constitutive equations in finite element codes. Computer Methods in Applied Mechanics and Engineering 141, 355–372.

Ganti, S., Parks, D., 1997. Elastic–plastic fracture mechanics of strength-mismatched interface cracks. In: Mahidhara, R.K., Geltmacher, A.B., Sadananda, K. (Eds.), Recent Advances in Fracture, TMS, pp. 13–25.

Hutchinson, J., 1968. Singular behaviour at the end of a tensile crack in a hardening material. J. Mech. Phys. Solids 16, 13–31.

Kim, A., Suresh, S., Shih, C.F., 1997. Fracture normal to layered and graded interfaces. Inter. J. Solids Structures 34 (26), 3415–3432.

O'Dowd, N., Shih, C.F., 1991. Family of crack-tip fields characterized by a triaxiality parameter—I. Structure of fields. J. Mech. Phys. Solids 39 (8), 989–1015.

O'Dowd, N., Shih, C.F., 1992. Family of crack-tip fields characterized by a triaxiality parameter—II. Fracture applications. J. Mech. Phys. Solids 40 (8), 939–963.

Ohata, M., Minami, F., Toyoda, M., 1996. Local approach to strength mis-match effect on cleavage fracture of notched material. In: Pineau, A., Rousselier, G. (Eds.), 1st European Mechanics of Materials Conference on Local Approach to Fracture EUROMECH-MECAMAT '96, pp. C6-269–C6-278.

Pineau, A., 1992. Global and local approaches to fracture-transferability of laboratory test results to components. In: Argon, A. (Ed.), Topics in Fracture and Fatigue. Springer-Verlag, New York, pp. 197–234.

Pineau, A., Joly, P., 1991. Local vs global approaches to elastic–plastic fracture mechanics. Application to ferritic steels and a cast duplex stainless steel. In: Blauel, J, Schwalbe, K. (Eds.). Defect Assessment in Components—Fundamentals and Applications, pp. 381–414. ESIS/ECF9.

Rice, J., 1968. A path independent integral and the approximate analysis of strain concentration by notches and cracks. J. Appl. Mech. 35, 379–386.

Rice, J., Rosengren, G., 1968. Plane strain deformation near a crack tip in a power-law hardening material. J. Mech. Phys. Solids 16, 1–12.

Rice, J., Tracey, D., 1969. On the enlargement of voids in triaxial stress fields. J. Mech. Phys. Sol. 17, 201–217.

Romeo, A., Ballarini, R., 1994. The influence of elastic mismatch on the size of the plastic zone of a crack terminating at a brittle–ductile interface. Int. J. of Fracture 65, 183–196.

Romeo, A., Ballarini, R., 1995. A crack very close to a bimaterial interface. J. Appl. Mech., 62, 614–619.

Shih, C., 1983. Tables of Hutchinson–Rice–Rosengren singular field quantities. Technical Report, MRL E-147. Brown University.

Sugimura, Y., Lim, P., Shih, C.F., Suresh, S., 1995. Fracture normal to a bimaterial interface: effects of plasticity on crack-tip shielding and amplification. Acta metall. mater. 43, 1157–1169.

Williams, M., 1959. The stresses around a fault or crack in dissimilar media. Bull Seis. Soc. Amer. 49, 199–204.

Woeltjen, C., Shih, C.F., Suresh, S., 1993. Cyclic near-tip fields for fatigue cracks along metal–metal and metal–ceramic interfaces. Acta metall. mater. 41, 2318–2335.

Zak, A., Williams, M., 1963. Crack point singularities at a bimaterial interface. J. Appl. Mech. 30, 142–143.